Published in final edited form as:
J Immunol. 2009 July 15; 183(2): 993–1004. doi:10.4049/jimmunol.0900803.

Immunomodulatory Function of Bone Marrow-Derived Mesenchymal Stem Cells in Experimental Autoimmune Type 1 Diabetes[1]

Paolo Fiorina[2,3,*,†], **Mollie Jurewicz**[2,*], **Andrea Augello**[‡], **Andrea Vergani**[*,†], **Shirine Dada**[*], **Stefano La Rosa**[‡], **Martin Selig**[¶], **Jonathan Godwin**[*], **Kenneth Law**[§], **Claudia Placidi**[‡], **R. Neal Smith**[¶], **Carlo Capella**[‡], **Scott Rodig**[§], **Chaker N. Adra**[*,‖], **Mark Atkinson**[#], **Mohamed H. Sayegh**[*], and **Reza Abdi**[3,*]

[*]Transplantation Research Center, Children's Hospital and Brigham and Women's Hospital, Harvard Medical School, Boston, MA 02115

[†]Department of Medicine, San Raffaele Scientific Institute, Milan, Italy

[‡]Department of Pathology, Ospedale di Circolo and Department of Human Morphology, University of Insubria, Varese, Italy

[§]Department of Pathology, Division of Hematopathology, Brigham and Women's Hospital, Boston, MA 02115

[¶]Department of Pathology, Massachusetts General Hospital, Boston, MA 02114

[‖]Stem Cell Therapy Program, King Faisal Specialist Hospital and Research Center, Riyadh, Kingdom of Saudi Arabia

[#]Department of Pathology, Immunology and Laboratory Medicine, University of Florida College of Medicine, Gainesville, FL 32610

Abstract

Human clinical trials in type 1 diabetes (T1D) patients using mesenchymal stem cells (MSC) are presently underway without prior validation in a mouse model for the disease. In response to this void, we characterized bone marrow-derived murine MSC for their ability to modulate immune responses in the context of T1D, as represented in NOD mice. In comparison to NOD mice, BALB/ c-MSC mice were found to express higher levels of the negative costimulatory molecule PD-L1 and to promote a shift toward Th2-like responses in treated NOD mice. In addition, transfer of MSC from resistant strains (i.e., nonobese resistant mice or BALB/c), but not from NOD mice, delayed the onset of diabetes when administered to prediabetic NOD mice. The number of BALB/c-MSC trafficking to the pancreatic lymph nodes of NOD mice was higher than in NOD mice provided autologous NOD-MSC. Administration of BALB/c-MSC temporarily

[1]This work is supported in part by National Institutes of Health P01 AI-41521, Juvenile Diabetes Research Foundation (JDRF) Grant 4-2007-1065, JDRF R&D Grant 4-2007-1065, and by the Scott and Heidi Schuster Foundation (M.H.S.). P.F. is the recipient of an American Society of Transplantation-JDRF Faculty Grant and a JDRF-Career Development Award. R.A. is the recipient of a JDRF Regular Grant.

[3]Address correspondence and reprint requests to Dr. Reza Abdi or Dr. Paolo Fiorina, Transplantation Research Center/Division of Nephrology, Brigham and Women's Hospital, Harvard Medical School, 221 Longwood Avenue, Boston, MA 02115. rabdi@rics.bwh.harvard.edu and paolo.fiorina@childrens.harvard.edu.
[2]P.F. and M.J. contributed equally to this work and are considered coauthors for this publication.

Disclosures
The authors have no financial conflict of interest.

resulted in reversal of hyperglycemia in 90% of NOD mice ($p = 0.002$). Transfer of autologous NOD-MSC imparted no such therapeutic benefit. We also noted soft tissue and visceral tumors in NOD-MSC-treated mice, which were uniquely observed in this setting (i.e., no tumors were present with BALB/c- or nonobese resistant mice-MSC transfer). The importance of this observation remains to be explored in humans, as inbred mice such as NOD may be more susceptible to tumor formation. These data provide important preclinical data supporting the basis for further development of allogeneic MSC-based therapies for T1D and, potentially, for other autoimmune disorders.

Mesenchymal stem cells (MSC)[4] are multipotent progenitor cells that can be isolated from a number of sources, including bone marrow (BM). MSC have been noted for their ability to give rise to cells of various lineages, including bone, cartilage, and adipose tissues (1). Isolation of MSC is commonly performed from BM, based on procedures involving the adherence of fibroblast-like cells to the plastic substrate of cell culture plates, together with the exclusion of marrow-derived hematopoietic cells (2, 3). MSC have been characterized in humans and several animal models using a battery of negative and positive cellular markers (3). Although subject to some discrepancy, a consensus opinion suggests they lack specific cell surface markers of hematopoietic cells (CD34), monocytes/macrophages (CD14), lymphocytes (CD11a/LFA-1), leukocytes (CD45), RBC (glycophorin A), and endothelial cells (CD31), but express SH2 (CD105 or endoglin), SH3, SH4, CD44, and CD29 (3–6). The primary impetus behind MSC research has been their developmental plasticity and ability to replace injured tissues, yet MSC have also been noted for their profound immunomodulatory effects in vivo (7, 8). Indeed, MSC have been used to reduce the burden of a variety of immune-mediated diseases, including graft rejection, graft-vs-host disease, collagen-induced arthritis, and myelin oligodendrocyte glycoprotein-induced experimental autoimmune encephalomyelitis (8–11). A significant number of trials have also been designed to assess the safety, feasibility, and efficacy of MSC therapy for a multitude of disorders in humans (12–14). Among these, Le Blanc et al. have shown promising results in using MSC for the treatment of steroid-refractory graft-vs-host disease in humans (15, 16). Clinical studies have also yielded success in treating common diseases such as cancer, heart failure from massive myocardial infarction, and neurological diseases (17–23). Taken collectively, these reports indicate that MSC may be of considerable therapeutic benefit and provide a basis for the development of efficacious and safe stem cell therapies (24). At least two clinical trials using allogeneic (Osiris) and autologous (European Consortium) MSC for therapy of recent onset type 1 diabetes (T1D) have recently been formed, without preclinical data (14). In this report, we characterize MSC obtained from diabetes-prone as well as -resistant mice, and evaluate their immunomodulatory effects in autoimmune T1D by assessing their ability to prevent the onset of diabetes, or to reverse overt hyperglycemia, in NOD mice.

Materials and Methods

Mice

BALB/c ByJ, NOD/LtJ, nonobese resistant mice (NOR)/LtJ, BDC2.5, CBA/J, and C57BL/6 mice were purchased from The Jackson Laboratory. Animals were cared for and/or bred under specific pathogen-free conditions at the Harvard Medical School Facilities for Animal Care and Housing. Protocols were approved by the Institutional Animal Care and Use Committee.

[4]Abbreviations used in this paper: MSC, mesenchymal stem cells; BM, bone marrow; DC, dendritic cell; NOR, nonobese resistant; P4, passage 4; PLN, pancreatic lymph node; T1D, type 1 diabetes; Treg, T regulatory cell.

MSC culture

To generate MSC, BM mononuclear cells were isolated from the femurs and tibiae of at least five mice to minimize cell variability. Cells were seeded in flasks at a concentration of $10 \times 10^6/25$ cm^2 in M10 medium (DMEM medium [Cambrex] containing 10% FCS [HyClone], 1% penicillin-streptomycin, and 1% L-glutamine [both from Cambrex]). To examine MSC in an inflammatory setting, 7.5×10^5 NOD- or BALB/c-MSC/well were cultured for 48 h in 6-well plates in M10 medium containing 10 ng/ml recombinant murine IL-1β (PeproTech).

Flow cytometric analysis

MSC were analyzed for surface expression of a battery of markers at passage 4 (P4). Anti-mouse Abs against CD45, Sca-1, CD44, CD90.2, CD73, CD80, CD86, CD40, CD40L, Fas, and FasL were purchased from BD Biosciences. Abs purchased from eBioscience were CD105, CD29, ICOS, OX40, PD-1, PD-L1, and PD-L2. T regulatory cells (Tregs) were assessed using CD4, CD25, and FoxP3 (eBioscience).

MSC differentiation

To ensure that our cultured cells had multipotent potential, we tested MSC P4 cultures for their ability to undergo differentiation into chondrocytes, osteocytes, and adipocytes as previously published (10). Chondrogenic differentiation was induced by 50 μg/ml ascorbic acid and 1 ng/ml TGFβ-1 (PeproTech); osteogenic differentiation was induced by 50 μg/ml ascorbic acid, 10 mM sodium α-glycerophosphate, and 10^{-8} M dexamethasone; adipogenic differentiation was induced by 10^{-7} M dexamethasone and 6 ng/ml insulin.

Immunohistochemistry and electron microscopy

Following fixation of adherent BALB/c- and NOD-MSC on slides using Merkofix (EMD Chemicals), MSC were incubated with primary Ab at 4°C overnight followed by the avidin-biotin complex procedure (25). Immunoreactions were employed using CD34, CD44, and CD105 (eBioscience) and Fas (Santa Cruz Biotechnology) abs. For electron microscopy, samples were fixed for 2 h in a solution of 2% paraformaldehyde and 2% glutar-aldehyde in 0.05 M pH 7.3 cacodylate buffer at 4°C

Islet pathology and immunohistochemistry

Immunohistology was performed as described previously (26).

Autoreactive T cell proliferation

T cells were extracted from spleens of BDC2.5 mice with CD4 magnetic beads (Miltenyi Biotec). Cells were then labeled using the Vybrant CFDA SE Cell Tracer kit (Invitrogen). Irradiated dendritic cells (DC; 5×10^4) from NOD mice were incubated with 1×10^5 CFSE-labeled CD4$^+$ BDC2.5 cells and 100 ng/ml BDC2.5 islet peptide as previously described (26). BALB/c- and NOD-MSC (2×10^4) irradiated with 3000 rad were added to assess the immunomodulatory effect on proliferation compared with control wells. At 72 h, cells were subjected to flow cytometric analysis to assess CFSE dilution.

Allogeneic MLR

DC (5×10^4) generated from C57BL/6 BM were harvested at day 8 and used to stimulate 1×10^5 CD4$^+$ BALB/c cells isolated using CD4 microbeads (Miltenyi Biotec). Irradiated BALB/c- and NOD-MSC (2×10^4) were added to determine their effect on T cell proliferation, in which cell counts were measured at day 3 following pulsing for 3 h with TdR (PerkinElmer) with a liquid scintillation counter.

ELISPOT

The effect of MSC on cytokine production of autoreactive T cells was examined with the ELISPOT assay using 1×10^5 $CD4^+$ BDC2.5 cells, 5×10^4 irradiated NOD DC, and 100 ng/ml BDC2.5 islet peptide for in vitro studies and 1×10^6 splenocytes with 100 μg/ml BDC2.5 islet peptide for ex vivo prevention studies to assess IFN-γ, IL-4, IL-6, and IL-10 as described previously (26).

Luminex assay

To assess cytokine production of murine serum and culture supernatant samples, a 21-plex cytokine kit (Millipore) was used according to the manufacturer's instructions to analyze production of indicated cytokines.

Prevention and reversal studies

To determine the effect of MSC administration on the prevention of diabetes, we injected 5×10^5 MSC (BALB/c or NOD) i.v. once a week for 4 wk in NOD mice beginning at 10 wk of age. Blood glucose measurements were performed by tail bleeding according to National Institutes of Health guidelines. For prevention studies, >250 mg glucose/dL for more than 3 days was indicative of greater than 80% loss of islet mass and onset of diabetes. For reversal studies, we placed a s.c. sustained-release insulin pellet (LinBit; LinShin Canada) on day 2 of hyperglycemia. Within 24 h of pellet placement, we performed the first MSC injection (1×10^6 cells i.v.). After all treatments, mice were monitored daily by blood glucose measurement until the time of sacrifice.

Gene array

RNA was isolated from MSC at P4 with the RNeasy kit (Qiagen) and was analyzed as previously described (26).

Trafficking studies

BALB/c- and NOD-MSC were harvested and labeled with CFSE as above. Cells were then injected into the tail vein of 10-wk-old female NOD mice. Age-matched, untreated NOD female mice were used to establish basal tissue autofluorescence. Animals were killed at day 3 postinjection. Spleen, pancreatic lymph nodes (PLN), and pancreata were removed, frozen in OCT and cut; 4-μm sections of the samples were examined to discern CFSE-labeled cells.

Results

MSC morphology and differentiation

To characterize our MSC colonies, MSC were generated from BM harvested from 10-wk-old female NOD and BALB/c mice and were evaluated morphologically by light and electron microscopy. Although BALB/c-MSC displayed a typical small spindle fibroblast-like pattern with eosinophilic cytoplasm and large clear nuclei showing dispersed chromatin and evident nucleoli, NOD-MSC formed large aggregates, primarily composed of packed, mid-sized to large cells, with rare spindle fibroblast-like cells (Fig. 1A). At the ultrastructural level, BALB/c-MSC showed more abundant cytoplasm with rare short microvilli compared with NOD-MSC (Fig. 1, E and F). By immunohistochemistry, both BALB/c- and NOD-MSC were observed to be negative for CD34 (Fig. 1B) and positive for CD44 (Fig. 1C) and CD105 (Fig. 1D), an expression pattern reported to identify MSC (14, 24). MSC cultured from NOD and BALB/c mice were able to differentiate into chondrocytes, osteocytes, and adipocytes (Fig. 1, G–I).

MSC flow cytometric characterization

We also evaluated the expression of stem cell and immunoregulatory markers by flow cytometry. NOD- and BALB/c-MSC were characterized at P4 with the following panel of Abs: 1) stem cell markers (CD29, CD44, CD73, CD105, CD166, and Sca-1); 2) hematopoietic/lineage markers (CD45 and CD90.2); 3) costimulatory molecules (positive: CD40, CD80, CD86, and OX40; negative: PD-1, PD-L1, and PD-L2); and 4) apoptotic factors (Fas and FasL). Stem cell marker expression was positive for CD29, CD44, CD73, CD105, CD166, and Sca-1 in both strains (Fig. 2, A, B, D, F, G, and H, respectively), although CD105 expression was lesser in NOD- than in BALB/c-MSC ($p = 0.001$; Fig. 2F). Neither BALB/c- nor NOD-MSC expressed lymphoid or myeloid markers (CD45 and CD90.2; Fig. 2, C and E). Positive costimulatory molecules appeared to be negative in both strains (Fig. 2, I–L), and the negative costimulatory molecules PD-1 and PD-L2 were not expressed in either strain (Fig. 2, M and O). However, PD-L1 expression was found to be 4-fold greater in BALB/c-MSC compared with NOD-MSC ($p = 0.01$; Fig. 2N). Although FasL was negative in both NOD- and BALB/c-MSC mice (Fig. 2Q), Fas (a receptor with proapoptotic properties) is expressed by both strains (Fig. 2P). We and others have previously shown that diabetes development is accelerated in NOD mice by treatment with a blocking PD-L1 Ab, as well as in PD-L1-deficient NOD mice (27, 28). Furthermore, Augello et al. demonstrated that MSC regulate the immune response in vitro through cell-to-cell contact, which appears to be largely dependent on the PD-1 pathway (29). We therefore further investigated the dynamic changes that occur in the expression of PD-L1 following MSC stimulation with IL-1β, thereby mimicking an in vivo inflammatory setting relative to T1D and based on the notion that the immunoregulatory characteristics of MSC most likely change in an inflammatory environment. Following challenge with IL-1β for 48 h, the difference in the expression of PD-L1 became more distinct in BALB/c-MSC (BALB/c = 21.0 ± 4.4 vs NOD = 5.4 ± 1.0%, $p = 0.024$; Fig. 2R). Altogether, a greater level of PD-L1 on BALB/c-MSC vs NOD-MSC may enable BALB/c-MSC to deliver immunosuppressive signals and to maintain quiescence of autoreactive T cells.

Cytokine profile of BALB/c- vs NOD-MSC and their immunosuppressive capabilities in alloimmune and autoimmune settings

To elucidate the regulatory function of MSC, we evaluated their production of inflammatory cytokines that may play a role in the pathogenesis of T1D, using the Luminex assay to analyze the supernatants of BALB/c- and NOD-MSC cultures at P4. Interestingly, NOD-MSC appeared to produce more proinflammatory cytokines and chemokines, including IL-1α ($p = 0.01$), IL-1β ($p = 0.04$), IP-10 ($p = 0.003$), and MCP-1 ($p = 0.007$) (Fig. 3A) than BALB/C-MSC did. No difference was noted in the levels of IFN-γ, IL-6, IL-9, IL-10, IL-12p40, IL-12p70, IL-15, MIG, or RANTES production. The immunosuppressive abilities of BALB/c- and NOD-MSC were also studied in an MLR assay. BALB/c- or NOD-MSC (2×10^4) were added, following irradiation with 3000 rad to prevent their proliferation in culture, to a fully mismatched MLR assay in which 1×10^5 C57BL/6 $CD4^+$ cells isolated from splenocytes were used as responders, with irradiated DC generated from CBA BM used as stimulators. MSC were therefore added as third-party cells. BALB/c- and NOD-MSC were both found to inhibit the MLR response in comparison to controls ($p < 0.001$), although BALB/c-MSC were noted to be more immunosuppressive ($p < 0.001$) in comparison to NOD-MSC (Fig. 3B). These findings confirm that both strains have similar immunosuppressive properties in an alloimmune setting in vitro. To evaluate the immunomodulatory abilities of MSC in an autoimmune setting in vitro, we used an autoreactive T cell proliferation assay shown to provide useful information with respect to T cell immunity to islet-cell Ags in T1D (26). The immunosuppressive properties of MSC were thus examined by assessing their effect on the proliferation of autoreactive T cells extracted from transgenic TCR BDC2.5 mice in response to autoantigen by CFSE dilution.

CFSE-labeled $CD4^+$ T cells purified from splenocytes of BDC2.5 mice were cultured for 3 days in the presence of BM-derived NOD DC, BALB/c- or NOD-MSC, and 100 ng/ml BDC2.5 peptide. As shown in Fig. 3C, both BALB/c- and NOD-MSC comparably inhibited the proliferative response of $CD4^+$ T cells ($p = 0.04$ compared with untreated control), demonstrating that both strains of MSC have similar immunomodulatory properties against autoreactive T cells in vitro.

Prevention of autoimmune diabetes in prediabetic NOD mice

We next tested the ability of P4 NOD- or BALB/c-MSC to prevent diabetes onset when injected into prediabetic NOD mice. Specifically, we injected 5×10^5 BALB/c- or NOD-MSC i.v. once a week for 4 wk into prediabetic 10-wk-old NOD mice ($n = 35$ for BALB/c-MSC, $n = 29$ for NOD-MSC, $n = 29$ for controls, $n = 3$ experiments). As shown in Fig. 4A, BALB/c-MSC ($p = 0.04$ compared with controls), but not NOD-MSC, significantly delayed the onset of T1D in 37% of treated NOD mice in the long-term (up to 40 wk of age) as compared with 20% of control NOD mice. In conjunction with the survival data, we also assessed the pathological finding of pancreatic islets in treated and control animals. Pancreatic islet morphology and infiltration were evaluated in MSC-treated or untreated NOD mice. Pancreata were harvested from normoglycemic NOD mice from the three groups (BALB/c-MSC-treated, NOD-MSC-treated, and untreated) at three different time points and were analyzed for infiltration and morphology ($n = 3$ mice/group). At 14 wk of age, islets appeared well-preserved in normoglycemic BALB/c-MSC-treated mice, while in normoglycemic NOD-MSC-treated or in untreated mice, a slightly more pronounced islet infiltration was observed (data not shown). At 22 wk of age, normoglycemic BALB/c-MSC-treated mice showed a scanty infiltrate, reduced in quantity to age-matched normoglycemic NOD-MSC-treated or untreated control mice (Fig. 4B, *1–3*, respectively). With respect to insulitis score, while BALB/c-MSC-treated mice showed a pattern similar to untreated 10-wk-old normoglycemic NOD mice, the insulitis score of BALB/c-MSC-treated mice was lower than that of age-matched NOD-MSC-treated and untreated NOD mice (Fig. 4C). Further investigation of the cell infiltrate subsets revealed fewer $CD3^+$ (Fig. 4B, *4–6*) and $B220^+$ cells (Fig. 4B, *10–12*) in BALB/c-MSC-treated mice compared with NOD-MSC-treated and untreated control mice. Very few $FoxP3^+$ cells were detected within the islets of all three groups of mice (Fig. 4B, *7–9*). Insulin (Fig. 4B, *13–15*) and glucagon (Fig. 4B, *16–18*) staining showed well-preserved islets, particularly in the BALB/c-MSC-treated group, whereas a loss of insulin staining and of islet morphology was evident in NOD-MSC-treated and untreated control mice. At 40 wk of age, normoglycemic BALB/c-MSC-treated mice maintained less infiltrated islets than NOD-MSC-treated and untreated control mice (data not shown). However, insulin staining appeared weak in BALB/c-MSC-treated mice and was negative in NOD-MSC-treated and untreated control mice, whereas glucagon was preserved in BALB/c-MSC-treated mice only (data not shown). Altogether, our data support the fact that BALB/c-MSC are capable of de-laying the onset of diabetes. These are vital preclinical data to support the concept of translating MSC-based cell therapy to individuals with T1D.

Evaluation of Th1 vs Th2 cytokine profile and measurement of Tregs following MSC treatment

The Th1 vs Th2 cytokine shift has also been reported to affect the incidence of T1D (30). We assessed the Th1/Th2 cytokine patterns in response to MSC treatment by stimulating splenocytes recovered with BDC2.5 peptide from control and treated animals, as previously described (26). Splenocytes of normoglycemic BALB/c- or NOD-MSC-treated and normoglycemic untreated control mice from our prevention studies were isolated at 14 wk of age (i.e., after 4 wk of treatment) and were challenged with BDC2.5 peptide in an ELISPOT assay to evaluate IFN-γ, IL-4, and IL-10 production. As shown in Fig. 4D, both BALB/c-

and NOD-MSC-treated animals exhibited a lower frequency of IFN-γ-producing cells than untreated normoglycemic NOD mice ($p = 0.01$ and $p = 0.005$ respectively for BALB/c- and NOD-MSC-treated mice). However, a shift toward a Th2 profile, with an increase in production of IL-4 ($p < 0.0001$ compared with controls) and IL-10 ($p = 0.01$ compared with controls), was evident in splenocytes isolated from BALB/c-MSC-treated mice. Such a shift was not observed in NOD-MSC-treated mice compared with control during autoantigen stimulation (Fig. 4D). Th2 cytokines have commonly been reported to confer protection against Th1-mediated destruction of β-islet cells (31).

Tregs have been shown to play a crucial role in regulating autoimmunity, (32, 33) and MSC have been shown to facilitate the generation of Tregs (34, 35). Upon examination of the effect of MSC treatment on Treg percentage, we noted a marginal but not substantial increase in the percentage of $CD4^+CD25^+FoxP3^+$ cells at 14 wk of age in the PLN of normoglycemic BALB/c-MSC-treated, but not of NOD-MSC-treated mice, compared with untreated age-matched controls (BALB/c-MSC-treated = 12.6 ± 0.8, untreated control = 10.0 ± 0.8, NOD-MSC-treated = 10.3 ± 1.1%, $p = 0.04$ BALB/c vs NOD-MSC-treated). No difference was observed in the percentage of Tregs recovered from the spleens of these mice (data not shown).

Reversal of hyperglycemia in newly hyperglycemic NOD mice

Given the protective effect of BALB/c-MSC observed in our prevention studies, we also evaluated the ability of BALB/c-MSC to reverse diabetes in new-onset hyperglycemic NOD mice. After a second consecutive hyperglycemic measurement (>250 mg/dl) within 24 h, NOD mice were injected i.v. with 1×10^6 BALB/c-MSC twice a week for 4 wk. An insulin pellet was placed under the skin of the dorsum of hyperglycemic NOD mice to improve glucose homeostasis. Although control NOD mice invariably returned to hyperglycemia (mean survival time = 22.5 days; Fig. 5, B and C), seven of eight BALB/c-MSC-treated mice remained normoglycemic for an average of 41.5 days ($p = 0.0002$ vs untreated mice; Fig. 5, A and C). Two BALB/c-MSC-treated mice remained normoglycemic for more than 60 days; one then reverted to hyperglycemia and the other died normoglycemic of unknown causes (Fig. 5, A and C). Despite the lack of therapeutic efficacy in our prevention studies using NOD-MSC, we tested the effect of NOD-MSC in reversing NOD mice with recent onset diabetes. In the three mice treated with NOD-MSC, none experienced reversal of their diabetes (Fig. 5B). Moreover, we observed tumor formation in all three hosts at the site of injection in the tail as well as at the site of the resident insulin pellet.

After 14 days of hyperglycemia in untreated NOD mice, islets are extensively infiltrated by lymphoid cells (Fig. 5D) with disrupted structure and a reduction in insulin and glucagon staining (data not shown). The lymphoid infiltrate was composed predominantly of $B220^+$ cells, along with a smaller population of $CD3^+$ cells (Fig. 5D) and very few $FoxP3^+$ cells (data not shown). In the BALB/c-MSC-treated mice 14 days after treatment, islets showed very mild infiltrates confined to the borders of β cells, with an almost complete absence of $B220^+$ and $CD3^+$ cells (Fig. 5E), along with well-maintained glucagon staining and scarce insulin staining (data not shown). More infiltrating cells also appeared to be $FoxP3^+$ cells in islets of the BALB/c-MSC-treated mice, which were absent in control mice (data not shown). In the long-term normoglycemic (i.e., 90 days after treatment) BALB/c-MSC-treated mice, islets still appeared preserved, despite a marked increase in infiltrate ($B220^+$ and $CD3^+$ cells) (Fig. 5F).

Occurrence of neoplasm in autologous MSC-treated mice

A paramount observation noted during our prevention and reversal studies was the identification of tumors in mice treated with autologous MSC. In prevention and reversal

groups, NOD mice treated with NOD-MSC developed neoplasia (~20% and 100%, respectively), a finding not observed in the BALB/c-MSC-treated group. Most tumors detected formed nodular masses in the legs and tails of mice (Fig. 6A). Tumors were also identified as numerous nodules of 0.1 to 0.3 cm in diameter in the lungs and liver of animals (Fig. 6, B and C). Optical microscopy revealed that the malignant tumor was made up of a homogeneous population of malignant spindle cells in sheets and fascicles (Fig. 6D). The tumor was shown to invade muscle, nerve, skin, bone (Fig. 6E), and peritoneum, and was located adjacent to the colon (Fig. 6F). In the lung, the tumor formed nodular masses with alveolar wall infiltration (Fig. 6G), and in the liver appeared as nodular masses (Fig. 6H). The tumor lacked malignant or benign-looking epithelium. Electron microscopy of the hepatic tumor identified compact, intertwined processes covered by basal lamina, consistent with Schwann cell differentiation (Fig. 6I). The diagnosis was compatible with a malignant peripheral nerve sheath tumor. Of note, following injection of BALB/c mice with BALB/c-MSC, no neoplasia was observed up to 5 wk after the initiation of treatment.

Transcriptome analysis of NOD- and BALB/c-MSC

Following culture and expansion of MSC (as above), mRNA was extracted from MSC for use in gene expression profile analysis using microarray technology. We examined the gene expression profile of NOD-MSC (samples no. 1 to 4) and BALB/c-MSC (samples no. 5 to 8) obtained from normoglycemic NOD mice and age-matched BALB/c mice. A striking differential expression in the pattern of gene regulation across the entire screen was observed when BALB/c-MSC genes were compared with the NOD-MSC (Fig. 6J). Notably, a considerable number of genes promoting cell cycle and proliferation were up-regulated in NOD-MSC (e.g., Plf2, Birc5, Ifgbp3, Sgol2, Btc, and Ccnb1); among these, Plf, Gfra1, and Ngef are related to neural tumor development, which is consistent with the pathogenesis behind the formation of neural tumors in our animals (Tables I and II, accession number GSE15516, http://www.ncbi.nlm.nih.gov/geo/query/acc.cgi?acc = GSE15516). Although the formation of tumors when using NOD-MSC could be due to an abnormality within the NOD strain similar to other genetic malformations reported in this strain, the data should raise awareness regarding the potential tumor formation in settings of autologous MSC in certain immune disorders (e.g., T1D).

Monitoring MSC trafficking following injection into NOD mice

MSC are able to selectively migrate into sites of injury (36). Furthermore, it has been shown that diabetogenic T cells are resident to the PLN, where T cells are introduced to β-cell autoantigens, giving rise to autoantigen-specific T cells (37). To study MSC trafficking in our experimental settings, BALB/c- as well as NOD-MSC were labeled with CFSE and were injected into the tail vein of 10-wk-old NOD mice. Pancreata, spleens, and PLN of treated and untreated animals were harvested at day 3 postinjection. As shown in Fig. 6, the frequency of trafficked cells was similar in both spleen and pancreas between BALB/ c-MSC-treated (Fig. 6, L and O, respectively) and NOD-MSC-treated mice (Fig. 6, M and P, respectively); however, a significant increase in the number of trafficked BALB/c-MSC was observed in the PLN as compared with NOD-MSC (Fig. 6, R and S, respectively). These data indicate that the prevention of diabetes observed with treatment of BALB/c-MSC could be due in part to the preferential trafficking of BALB/c-MSC to the PLN, where they may interfere or deliver inhibitory signals to prevent the expansion of autoreactive T cells. Chemokines have increasingly become recognized as the key regulators of such preferential migration of cells, including MSC (38). It is likely that the disparity in the migration of MSC from these two strains could be due to the differential expression of chemokine receptors. We therefore assessed the expression of chemokine receptors CCR5, CCR7, CXCR3, and CXCR4 on MSC by FACS. The expression of CXCR3 and CCR7 was significantly higher on BALB/c-MSC in comparison to NOD-MSC (Fig. 6T). Interestingly,

CXCR3 has in particular been associated with the migration of autoreactive T cells into the PLN in the presence of high gradients of IP-10 (CXCL-10) in the PLN (39).

Prevention of diabetes by MSC isolated from NOR mice

It could be argued that the preventive effect we observed in the case of BALB/c-MSC was due to the activation of immune responses by allogeneic cells. To examine the effect of MSC from a strain more similar to NOD, we isolated MSC from NOR mice. NOR is a diabetes-resistant strain with ∼90% genomic identity with NOD mice. NOR share, for instance, the MHC class II molecule of NOD mice, including the diabetogenic H-2g7 complex (40). For this effort, 5×10^5 MSC were injected into prediabetic female NOD mice (10 wk of age) once a week for 4 wk, a strategy identical with treatments using BALB/c- and NOD-MSC. As shown in Fig. 7A, delivery of NOR-MSC to prediabetic NOD mice was able to prevent diabetes. Furthermore, histological analysis of the pancreas harvested from NOR-MSC-treated mice at 30 wk posttreatment showed preserved islets with substantial insulin staining and minimal cellular infiltrate (Fig. 7B). Importantly, similar to BALB/c-MSC treated mice, we did not observe any tumor development in NOR-MSC-treated recipients.

Discussion

The incidence of T1D continues to climb steadily, making it one of the most challenging health issues of the 21st century worldwide (41). In addition, the morbidity and mortality associated with diabetes are constantly rising and are anticipated to remain a problem for years to come (41, 42). The use of immunosuppressants to reverse or halt diabetes has received much attention, but the shortfall of monotherapy and serious morbidity from lifelong immunosuppression has prompted investigators to search for alternative approaches. Investigators have begun to use MSC much more quickly than other cell-based therapies in a variety of human diseases. Interestingly, administration of MSC in many of these settings has offered significant benefits with no major adverse effects. Although MSC plasticity is a propitious feature of the cell and has been used as a rationale to develop clinical trials (http://clinicaltrials.gov; see Refs. 17–23), the immunomodulatory effects of MSC have recently become of interest as well (11, 12, 14, 24).

Our data in this study show that allogeneic MSC are capable of protecting islet mass and of delaying the onset of disease when injected into prediabetic NOD mice. Administration of allogeneic BALB/c-MSC also showed promising results in temporarily reversing hyperglycemia in new-onset diabetic NOD mice. These novel data indicate that MSC could be a component of an innovative and successful cell-based regimen for T1D treatment on its own. An important lesson from intervention therapies in T1D is that monotherapy often fails to provide a durable favorable outcome, particularly for reversal of the disease. In theory, MSC therapy could allow investigators to use lesser amounts of immunosuppressive agents, which, as previously noted, have been shown to carry a high degree of toxicity. Although the hypoimmunogenicity of allogeneic MSC is certainly of value, MSC are reported to be efficiently recognized by the host immune response and eventually are rejected (43). The lack of a long-term effect of BALB/ c-MSC may be related to this recognition and subsequent rejection. Therefore, future studies should focus on understanding the life span of MSC and the value of repeated administration for a longer period of time. Additional research is also needed to identify various synergistic immunosuppressive strategies and to optimize prevention and reversal of established diabetes. Given that this strategy requires the generation of large numbers of MSC, these studies will certainly represent a considerable undertaking. Although the use of MSC comprises an exciting therapeutic approach for T1D, translating our results to the clinic requires greater investigation to provide robust preclinical data to safely and effectively use MSC as a cell-based therapy for T1D.

Our data demonstrating the similarity in the ability of BALB/c-and NOD-MSC to suppress the T cell response in vitro is in accordance with data using MSC from healthy individuals and from patients with autoimmune diseases such as scleroderma and rheumatoid arthritis in which comparable suppression of T cell proliferation was achieved in vitro (44). Given the disparity we observed in the in vivo effects of NOD- and BALB/c-MSC in regulating diabetes, we further examined MSC from these two strains to explain the outcome differences noted in our studies. Although as previously stated, both strains of MSC were able to suppress alloimmune and autoimmune responses, several intrinsic differences were evident between them. First, an increased growth rate of NOD-MSC as compared with BALB/c-MSC was observed as well as a resultant production of a proinflammatory or diabetogenic cytokine profile. Gene arrays confirm the presence of two distinct gene profiles, with NOD-MSC expressing more proinflammatory genes compared with BALB/c-MSC. Furthermore, ultrastructural analysis with electron microscopy revealed differences in intracytoplasmic organelles and pseudopods, which may have an impact on cell-to-cell interactions as well as on cell trafficking. Interestingly, the expression of PD-L1, a major regulatory molecule in T1D, was much greater in BALB/c-MSC, which may serve as a potential mechanism by which BALB/c-MSC exert their suppressive effect on autoreactive T cells in vivo (45). Following injection of MSC, we did observe an increase in the percentage of Tregs and Th2 cytokines, both of which have been shown to be protective in T1D (32, 33, 46, 47). A key feature of MSC is their ability to selectively migrate into sites of injury. Moreover, it has been shown that diabetogenic T cells are generated in the PLN, where they are introduced to Ags by DC. The preferential recruitment of BALB/c-MSC to the lymph node, along with high levels of PD-L1 expression on BALB/c-MSC, supports the idea that these cells could directly suppress autoreactive T cells in vivo. Our chemokine expression studies of MSC suggest a preferential expression of specific chemokine receptors on BALB/c-MSC, which correlates with the postulation that by inhibiting or stimulating chemokines/receptors, it will be possible to promote the homing of MSC to specific anatomical sites to achieve the desired therapeutic effects (36). It is known that immunoregulatory effects of MSC are exerted through different putative mechanisms, including immune cell interaction, production of soluble factors, and promotion of Treg generation (14). These mechanisms are most likely not mutually exclusive, and future studies should examine their relative contributions to the immunomodulatory functions of MSC. It should be noted that given the plasticity of MSC, transdifferentia-tion of autologous MSC could occur; however, because NOD-MSC were observed to have no effect in our prevention studies, the possibility of MSC differentiation into islets for example seems unlikely. Nevertheless, this requires additional experiments beyond the scope of the present study.

We observed rapidly growing tumors in mice treated with autologous MSC. Tumors were detected in the liver and lungs of our injected mice, where a large number of MSC are retained after i.v. injection. The incidence of tumor formation was higher in the reversal group, most likely due to the more intense administration regimen of NOD-MSC in the reversal group compared with the prevention group. Inbred mice such as NOD have been shown to carry various genetic abnormalities and are prone to developing lymphoid tumors, therefore it remains to be elucidated whether autologous MSC indeed pose a risk, whether the observed tumor formation is related to NOD abnormalities, or whether it has any clinical implication for humans (48). At present, tumor formation following use of autologous MSC has not been demonstrated to be a major impediment to current clinical trials, although this has not been studied in the context of T1D. Nevertheless, it is important to impart this message to any studies aiming to use autologous MSC to treat the disease of interest (49). The lack of tumor formation in the case of allogeneic BALB/c-MSC could be due to their recognition by the host immunosurveillance, ensuring that their proliferation is controlled. Moreover, NOD-MSC were unable to exhibit any effect on the prevention of diabetes. Lack

of tumor formation using our NOR-MSC, along with a simultaneous effect on suppressing diabetes, may argue in favor of using MSC from diabetes-resistant siblings. In summary, we believe our data provide a basis for the development of a cell-based therapy for which MSC from nondiabetic donors could be isolated and administered to patients for the prevention and reversal of T1D. Indeed, the translation of this knowledge into clinical practice could eventually transform the overall strategy we use to treat this disease.

Acknowledgments

Microarray studies were performed by the Molecular Genetics Core Facility at Children's Hospital Boston.

References

1. Oswald J, Boxberger S, Jorgensen B, Feldmann S, Ehninger G, Bornhäuser M, Werner C. Mesenchymal stem cells can be differentiated into endothelial cells in vitro. Stem Cells. 2004; 22:377–384. [PubMed: 15153614]
2. Friedenstein AJ, Piatetzky-Shapiro II, Petrakova KV. Osteo-genesis in transplants of bone marrow cells. J. Embryol. Exp. Morphol. 1966; 16:381–390. [PubMed: 5336210]
3. Pittenger MF, Mackay AM, Beck SC, Jaiswal RK, Douglas R, Mosca JD, Moorman MA, Simonetti DW, Craig S, Marshak DR. Multilineage potential of adult human mesenchymal stem cells. Science. 1999; 284:143–147. [PubMed: 10102814]
4. Jorgensen C, Djouad F, Apparailly F, Noel D. Engineering mes-enchymal stem cells for immunotherapy. Gene Ther. 2003; 10:928–931. [PubMed: 12732877]
5. Jorgensen C, Djouad F, Fritz V, Apparailly F, Plence P, Noel D. Mesenchymal stem cells and rheumatoid arthritis. Joint Bone Spine. 2003; 70:483–485. [PubMed: 14667559]
6. Kassis I, Zangi L, Rivkin R, Levdansky L, Samuel S, Marx G, Gorodetsky R. Isolation of mesenchymal stem cells from G-CSF-mobi-lized human peripheral blood using fibrin microbeads. Bone Marrow Transplant. 2006; 37:967–976. [PubMed: 16670702]
7. Djouad F, Plence P, Bony C, Tropel P, Apparailly F, Sany J, Noe¨l D, Jorgensen C. Immunosuppressive effect of mesenchymal stem cells favors tumor growth in allogeneic animals. Blood. 2003; 102:3837–3844. [PubMed: 12881305]
8. Ryan JM, Barry FP, Murphy JM, Mahon BP. Mesenchymal stem cells avoid allogeneic rejection. J. Inflamm. (Lond.). 2005; 2:8. [PubMed: 16045800]
9. Bartholomew A, Sturgeon C, Siatskas M, Ferrer K, McIntosh K, Patil S, Hardy W, Devine S, Ucker D, Deans R, Moseley A, Hoffman R. Mesenchymal stem cells suppress lymphocyte proliferation in vitro and prolong skin graft survival in vivo. Exp. Hematol. 2002; 30:42–48. [PubMed: 11823036]
10. Augello A, Tasso R, Negrini SM, Cancedda R, Pennesi G. Cell therapy using allogeneic bone marrow mesenchymal stem cells prevents tissue damage in collagen-induced arthritis. Arthritis Rheum. 2007; 56:1175–1186. [PubMed: 17393437]
11. Zappia E, Casazza S, Pedemonte E, Benvenuto F, Bonanni I, Gerdoni E, Giunti D, Ceravolo A, Cazzanti F, Frassoni F, Mancardi G, Uccelli A. Mesenchymal stem cells ameliorate experimental autoimmune encephalomyelitis inducing T-cell anergy. Blood. 2005; 106:1755–1761. [PubMed: 15905186]
12. Le Blanc K, Ringden O. Immunomodulation by mesenchymal stem cells and clinical experience. J. Intern. Med. 2007; 262:509–525. [PubMed: 17949362]
13. Ozaki K, Sato K, Oh I, Meguro A, Tatara R, Muroi K, Ozawa K. Mechanisms of immunomodulation by mesenchymal stem cells. Int. J. Hematol. 2007; 86:5–7. [PubMed: 17675259]
14. Abdi R, Fiorina P, Adra CN, Atkinson M, Sayegh MH. Immunomodulation by mesenchymal stem cells: a potential therapeutic strategy for type 1 diabetes. Diabetes. 2008; 57:1759–1767. [PubMed: 18586907]
15. Le Blanc K, Rasmusson I, Sundberg B, Gotherstrom C, Hassan M, Uzunel M, Ringden O. Treatment of severe acute graft-versus-host disease with third party haploidentical mesenchymal stem cells. Lancet. 2004; 363:1439–1441. [PubMed: 15121408]

16. Ringden O, Uzunel M, Rasmusson I, Remberger M, Sundberg B, Lonnies H, Marschall HU, Dlugosz A, Szakos A, Hassan Z, et al. Mesenchymal stem cells for treatment of therapy-resistant graft-versus-host disease. Transplantation. 2006; 81:1390–1397. [PubMed: 16732175]
17. Stamm C, Liebold A, Steinhoff G, Strunk D. Stem cell therapy for ischemic heart disease: beginning or end of the road? Cell Transplant. 2006; 15:S47–S56. [PubMed: 16826795]
18. Numaguchi Y, Sone T, Okumura K, Ishii M, Morita Y, Kubota R, Yokouchi K, Imai H, Harada M, Osanai H, Kondo T, Murohara T. The impact of the capability of circulating progenitor cell to differentiate on myocardial salvage in patients with primary acute myocardial infarction. Circulation. 2006; 114:I114–I119. [PubMed: 16820559]
19. Mazzini L, Mareschi K, Ferrero I, Vassallo E, Oliveri G, Boccaletti R, Testa L, Livigni S, Fagioli F. Autologous mesenchymal stem cells: clinical applications in amyotrophic lateral sclerosis. Neurol. Res. 2006; 28:523–526. [PubMed: 16808883]
20. Le Blanc K, Ringden O. Mesenchymal stem cells: properties and role in clinical bone marrow transplantation. Curr. Opin. Immunol. 2006; 18:586–591. [PubMed: 16879957]
21. Behfar A, Terzic A. Derivation of a cardiopoietic population from human mesenchymal stem cells yields cardiac progeny. Nat. Clin. Pract. Car-diovasc. Med. 2006; 3:S78–S82.
22. Chen LB, Jiang XB, Yang L. Differentiation of rat marrow mesenchymal stem cells into pancreatic islet β-cells. World J. Gastroenterol. 2004; 10:3016–3020. [PubMed: 15378785]
23. Koc ON, Day J, Nieder M, Gerson SL, Lazarus HM, Krivit W. Allogeneic mesenchymal stem cell infusion for treatment of metachromatic leukodystrophy (MLD) and Hurler syndrome (MPS-IH). Bone Marrow Transplant. 2002; 30:215–222. [PubMed: 12203137]
24. Uccelli A, Moretta L, Pistoia V. Mesenchymal stem cells in health and disease. Nat. Rev. Immunol. 2008; 8:726–736. [PubMed: 19172693]
25. Hsu SM, Raine L, Fanger H. Use of avidin-biotin-peroxidase complex (ABC) in immunoperoxidase techniques: a comparison between ABC and unlabeled antibody (PAP) procedures. J. Histochem. Cytochem. 1981; 29:577–580. [PubMed: 6166661]
26. Fiorina P, Vergani A, Dada S, Jurewicz M, Wong M, Law K, Wu E, Tian Z, Abdi R, Guleria I, et al. Targeting CD22 reprograms B-cells and reverses autoimmune diabetes. Diabetes. 2008; 57:3013–3024. [PubMed: 18689692]
27. Ansari MJ, Salama AD, Chitnis T, Smith RN, Yagita H, Akiba H, Yamazaki T, Azuma M, Iwai H, Khoury SJ, Auchincloss H Jr, Sayegh MH. The programmed death-1 (PD-1) pathway regulates autoimmune diabetes in nonobese diabetic (NOD) mice. J. Exp. Med. 2003; 198:63–69. [PubMed: 12847137]
28. Keir ME, Liang SC, Guleria I, Latchman YE, Qipo A, Albacker LA, Koulmanda M, Freeman GJ, Sayegh MH, Sharpe AH. Tissue expression of PD-L1 mediates peripheral T cell tolerance. J. Exp. Med. 2006; 203:883–895. [PubMed: 16606670]
29. Augello A, Tasso R, Negrini SM, Amateis A, Indiveri F, Cancedda R, Pennesi G. Bone marrow mesenchymal progenitor cells (BMSC) inhibit lymphocyte proliferation by activation of the programmed death 1 (PD-1) pathway. Eur. J. Immunol. 2005; 35:1482–1490. [PubMed: 15827960]
30. Papaccio G, Pisanti FA, Montefiano RD, Graziano A, Latronico MV. Th1 and Th2 cytokines exert regulatory effects upon islet microvascular areas in the NOD mouse. J. Cell. Biochem. 2002; 86:651–664. [PubMed: 12210732]
31. Azar ST, Tamim H, Beyhum HN, Habbal MZ, Almawi WY. Type I (insulin-dependent) diabetes is a Th1- and Th2-mediated autoimmune disease. Clin. Diagn. Lab. Immunol. 1999; 6:306–310. [PubMed: 10225827]
32. Tarbell KV, Petit L, Zuo X, Toy P, Luo X, Mqadmi A, Yang H, Suthanthiran M, Mojsov S, Steinman RM. Dendritic cell-expanded, islet-specific CD4+ CD25+ CD62L+ regulatory T cells restore normoglycemia in diabetic NOD mice. J. Exp. Med. 2007; 204:191–201. [PubMed: 17210729]
33. Tonkin DR, He J, Barbour G, Haskins K. Regulatory T cells prevent transfer of type 1 diabetes in NOD mice only when their antigen is present in vivo. J. Immunol. 2008; 181:4516–4522. [PubMed: 18802054]

34. Gonzalez-Rey E, Gonzalez MA, Varela N, O'Valle F, Hernandez-Cortes P, Rico L, Buscher D, Delgado M. Human adipose-derived mesenchymal stem cells reduce inflammatory and T-cell responses and induce regulatory T cells in vitro in rheumatoid arthritis. Ann. Rheum Dis. 2009 In press.
35. Casiraghi F, Azzollini N, Cassis P, Imberti B, Morigi M, Cugini D, Cavinato RA, Todeschini M, Solini S, Sonzogni A, et al. Pretransplant infusion of mesenchymal stem cells prolongs the survival of a semiallogeneic heart transplant through the generation of regulatory T cells. J. Immunol. 2008; 181:3933–3946. [PubMed: 18768848]
36. Sackstein R, Merzaban JS, Cain DW, Dagia NM, Spencer JA, Lin CP, Wohlgemuth R. Ex vivo glycan engineering of CD44 programs human multipotent mesenchymal stromal cell trafficking to bone. Nat. Med. 2008; 14:181–187. [PubMed: 18193058]
37. Gagnerault MC, Luan JJ, Lotton C, Lepault F. Pancreatic lymph nodes are required for priming of β cell reactive T cells in NOD mice. J. Exp. Med. 2002; 196:369–377. [PubMed: 12163565]
38. Chamberlain G, Wright K, Rot A, Ashton B, Middleton J. Murine mesenchymal stem cells exhibit a restricted repertoire of functional chemokine receptors: comparison with human. PLoS ONE. 2008; 3:e2934. [PubMed: 18698345]
39. Christen U, Benke D, Wolfe T, Rodrigo E, Rhode A, Hughes AC, Oldstone MB, von Herrath MG. Cure of prediabetic mice by viral infections involves lymphocyte recruitment along an IP-10 gradient. J. Clin. Invest. 2004; 113:74–84. [PubMed: 14702111]
40. Prochazka M, Serreze DV, Frankel WN, Leiter EH. NOR/Lt mice: MHC-matched diabetes-resistant control strain for NOD mice. Diabetes. 1992; 41:98–106. [PubMed: 1727742]
41. Schatz D, Gale EA, Atkinson MA. Why can't we prevent type 1 diabetes?: maybe it's time to try a different combination. Diabetes Care. 2003; 26:3326–3328. [PubMed: 14633822]
42. von Herrath M, Sanda S, Herold K. Type 1 diabetes as a relapsing-remitting disease? Nat. Rev. Immunol. 2007; 7:988–994. [PubMed: 17982429]
43. Nauta AJ, Westerhuis G, Kruisselbrink AB, Lurvink EG, Willemze R, Fibbe WE. Donor-derived mesenchymal stem cells are immunogenic in an allogeneic host and stimulate donor graft rejection in a nonmyeloablative setting. Blood. 2006; 108:2114–2120. [PubMed: 16690970]
44. Bocelli-Tyndall C, Bracci L, Spagnoli G, Braccini A, Bouchenaki M, Ceredig R, Pistoia V, Martin I, Tyndall A. Bone marrow mesenchymal stromal cells (BM-MSCs) from healthy donors and auto-immune disease patients reduce the proliferation of autologous- and allogeneic-stimulated lymphocytes in vitro. Rheumatology (Oxford). 2007; 46:403–408. [PubMed: 16920750]
45. Ansari MJ, Salama AD, Chitnis T, Smith RN, Yagita H, Akiba H, Yamazaki T, Azuma M, Iwai H, Khoury SJ, Auchincloss H Jr, Sayegh MH. The programmed death-1 (PD-1) pathway regulates autoimmune diabetes in nonobese diabetic (NOD) mice. J. Exp. Med. 2003; 198:63–69. [PubMed: 12847137]
46. Sia C. Imbalance in Th cell polarization and its relevance in type 1 diabetes mellitus. Rev. Diabet. Stud. 2005; 2:182–186. [PubMed: 17491692]
47. Tian J, Clare-Salzler M, Herschenfeld A, Middleton B, Newman D, Mueller R, Arita S, Evans C, Atkinson MA, Mullen Y, et al. Modulating autoimmune responses to GAD inhibits disease progression and prolongs islet graft survival in diabetes-prone mice. Nat. Med. 1996; 2:1348–1353. [PubMed: 8946834]
48. Chiu PP, Ivakine E, Mortin-Toth S, Danska JS. Susceptibility to lymphoid neoplasia in immunodeficient strains of nonobese diabetic mice. Cancer Res. 2002; 62:5828–5834. [PubMed: 12384545]
49. Tolar J, Nauta AJ, Osborn MJ, Mortari APanoskaltsis, McElmurry RT, Bell S, Xia L, Zhou N, Riddle M, Schroeder TM, et al. Sarcoma derived from cultured mesenchymal stem cells. Stem Cells. 2007; 25:371–379. [PubMed: 17038675]

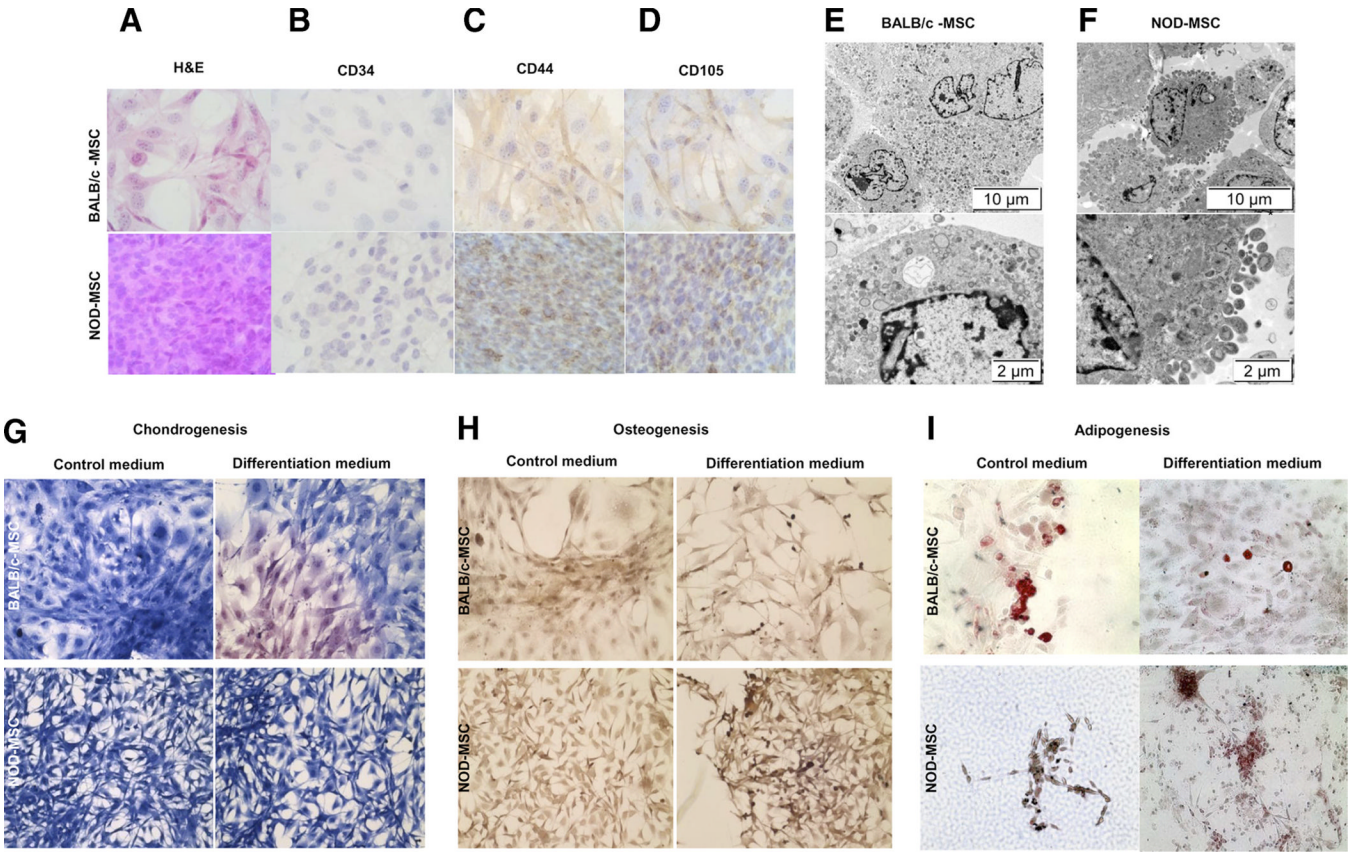

FIGURE 1.

MSC characterization and differentiation. Although BALB/c-MSC primarily displayed a fibroblastic pattern, NOD-MSC grew in large aggregates formed by packed, round to oval, mid-sized to large cells, with only rare spindle fibroblast-like cells (*A*). Both MSC were negative for CD34 and immunoreactive for CD44 and CD105 (*B–D*) (magnification: ×400 for BALB/c-MSC and ×250 for NOD-MSC). Upon examination by electron microscopy, BALB/c-MSC appeared as large cells with abundant cytoplasm and smooth cell surfaces with rare microvilli. Nuclei were irregular with predominant central euchromatin and scarce peripheral heterochromatin (*E*). NOD-MSC showed scarce cytoplasm but prominent surface microvilli, with some dilated rough endoplasmic cisternae, mitochondria, and sparse lysosomes with irregular nuclei, scarce peripheral heterochromatin, and some nucleoli (*F*). Sections were examined using a Philips Morgagni electron microscope. To examine their "stemness," we tested MSC cultures for their capacity to differentiate into other cell lineages. MSC from NOD and BALB/c mice were able to differentiate into chondrocytes (*G*), osteocytes (*H*), and adipocytes (*I*), shown using ×400 magnification.

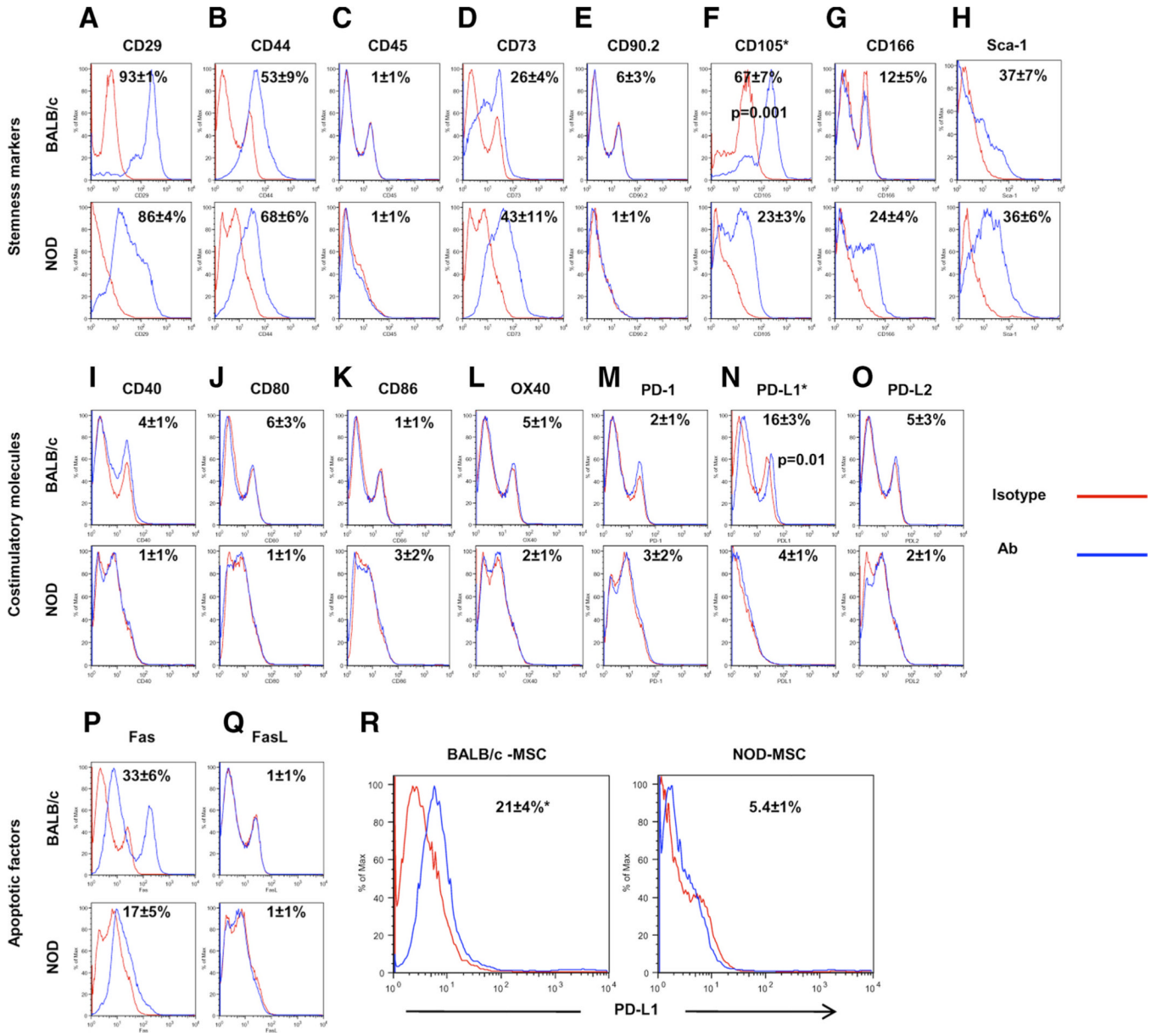

FIGURE 2.

Assessment of MSC for stem cell and immunomodulatory markers by FACS. Stem cell markers, costimulatory molecules, and apoptotic factors were evaluated in MSC at P4 by FACS analysis ($n = 3$ experiments). The stem cell markers CD29 (*A*), CD44 (*B*), CD73 (*D*), CD105 (*F*), CD166 (*G*), and Sca-1 (*H*) were positive in NOD- and BALB/c-MSC, with CD105 expression higher in BALB/c-MSC compared with NOD-MSC ($p = 0.001$). Myeloid markers such as CD45 (*C*) and CD90.2 (*E*) were negative in both strains of MSC. Most positive costimulatory molecules appeared to be negative or were expressed at very low levels in both strains (*I–L*). Among negative costimulatory molecules, PD-1 and PD-L2 were not expressed in either strain of MSC (*M* and *O*), while PD-L1 was more expressed in BALB/c-MSC compared with NOD-MSC ($p = 0.01$) (*N*). FasL was negative in both NOD- and BALB/c-MSC (*Q*), but Fas was expressed by both strains (*P*). MSC were also challenged for 48 h with IL-1β. In BALB/c-MSC, but not in NOD-MSC, the expression of PD-L1 increased (BALB/c-MSC vs NOD-MSC, $p = 0.024$) (*R*).

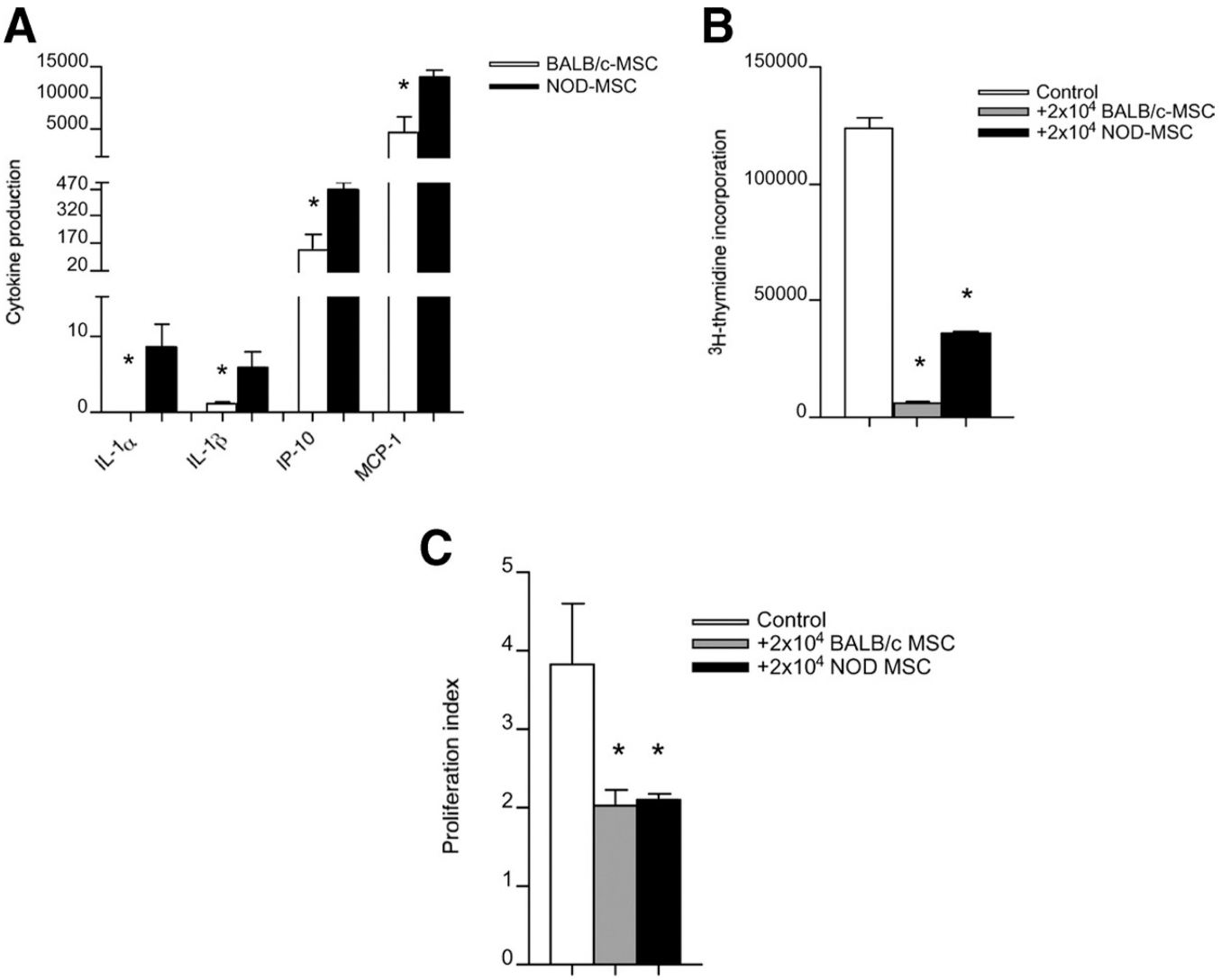

FIGURE 3.

Cytokine profile of BALB/c- vs NOD-MSC and their ability to suppress allogeneic and autoantigen-specific T cell proliferation. *A*, NOD-MSC produced higher levels of proinflammatory cytokines/ chemokines including IL-1α ($p = 0.01$), IL-1β ($p = 0.04$), IP-10 ($p = 0.003$), and MCP-1 ($p = 0.007$) (mean of duplicate wells/experiment, four experiments). *B*, Both BALB/c- and NOD-MSC were found to inhibit the MLR response compared with control ($p < 0.001$), although BALB/c-MSC were more potent in their ability to abrogate allogeneic T cell proliferation ($p < 0.001$ compared with NOD-MSC). *C*, BALB/c- and NOD-MSC similarly inhibited the proliferation of autoreactive T cells extracted from transgenic BDC2.5 mice in response to autoantigen by CFSE dilution ($p = 0.04$) (as calculated by proliferation index, mean of triplicate wells, representative of two experiments).

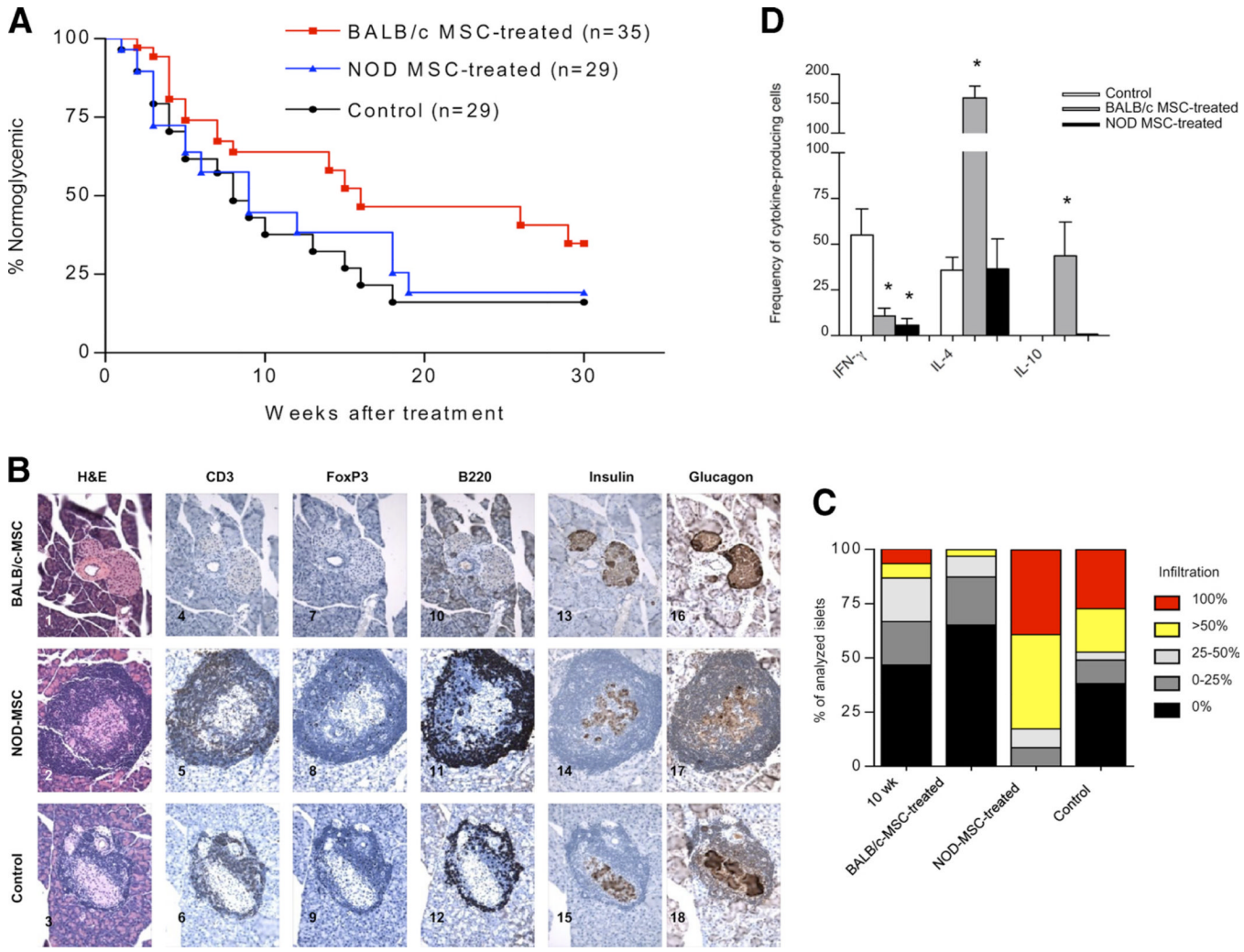

FIGURE 4.

Prevention of diabetes by BALB/c-MSC in NOD mice. BALB/c-MSC or NOD-MSC (5×10^5) were injected i.v. once a week for 4 wk into prediabetic 10-wk-old NOD mice ($n = 35$ mice for BALB/c-MSC, $n = 28$ mice for NOD-MSC, $n = 3$ experiments). *A*, BALB/c-MSC ($p = 0.04$ compared with controls), but not NOD-MSC, significantly delayed the onset of T1D in 37% of treated NOD mice in the long-term (up to 40 wk of age). *B*, At 22 wk of age, pancreata from normoglycemic BALB/c-MSC-treated mice showed a scanty infiltrate compared with NOD-MSC-treated and untreated controls (*1*, *2*, and *3*, respectively) with very few $CD3^+$(*4–6*) and $B220^+$ cells (*10–12*), which conversely infiltrated the islets of NOD-MSC-treated and untreated controls. *7–9*, Very few $FoxP3^+$ cells were detected within the islets of all three groups of mice. Insulin (*13–15*) and glucagon (*16–18*) staining showed well-preserved islets, particularly in the BALB/c-MSC-treated mice, whereas a loss of insulin staining and islet morphology was evident in NOD-MSC-treated or untreated mice. *C*, At 22 wk of age, BALB/c-MSC-treated NOD mice showed a lower insulitis score than age-matched normoglycemic NOD-MSC-treated or untreated control mice, and BALB/c-MSC-treated mice showed a similar pattern of insulitis as untreated 10-wk-old normoglycemic NOD mice. Insulitis was scored by counting at least 50 islets/mouse from at least three mice/group. Photomicrographs were taken on an Olympus BX41 microscope at indicated magnifications using an Olympus Q-color5 digital camera and analyzed with

Adobe Photoshop Elements 2.0. All photos were taken at ×400 original magnification. *D*, Assessment of Th1 vs Th2 cytokine shift. Splenocytes of normoglycemic BALB/c- or NOD-MSC-treated and normoglycemic untreated control mice were isolated at 14 wk of age and were challenged with the BDC2.5 peptide in an ELISPOT assay to evaluate cytokine production. A reduction in IFN-γ production was evident for BALB/c-MSC- ($p = 0.01$) and NOD-MSC-treated mice ($p = 0.005$). The production of Th2 cytokines (IL-4 [$p < 0.0001$] and IL-10 [$p = 0.01$]) was higher in BALB/c-MSC-treated mice (but not in NOD-MSC-treated) compared with controls.

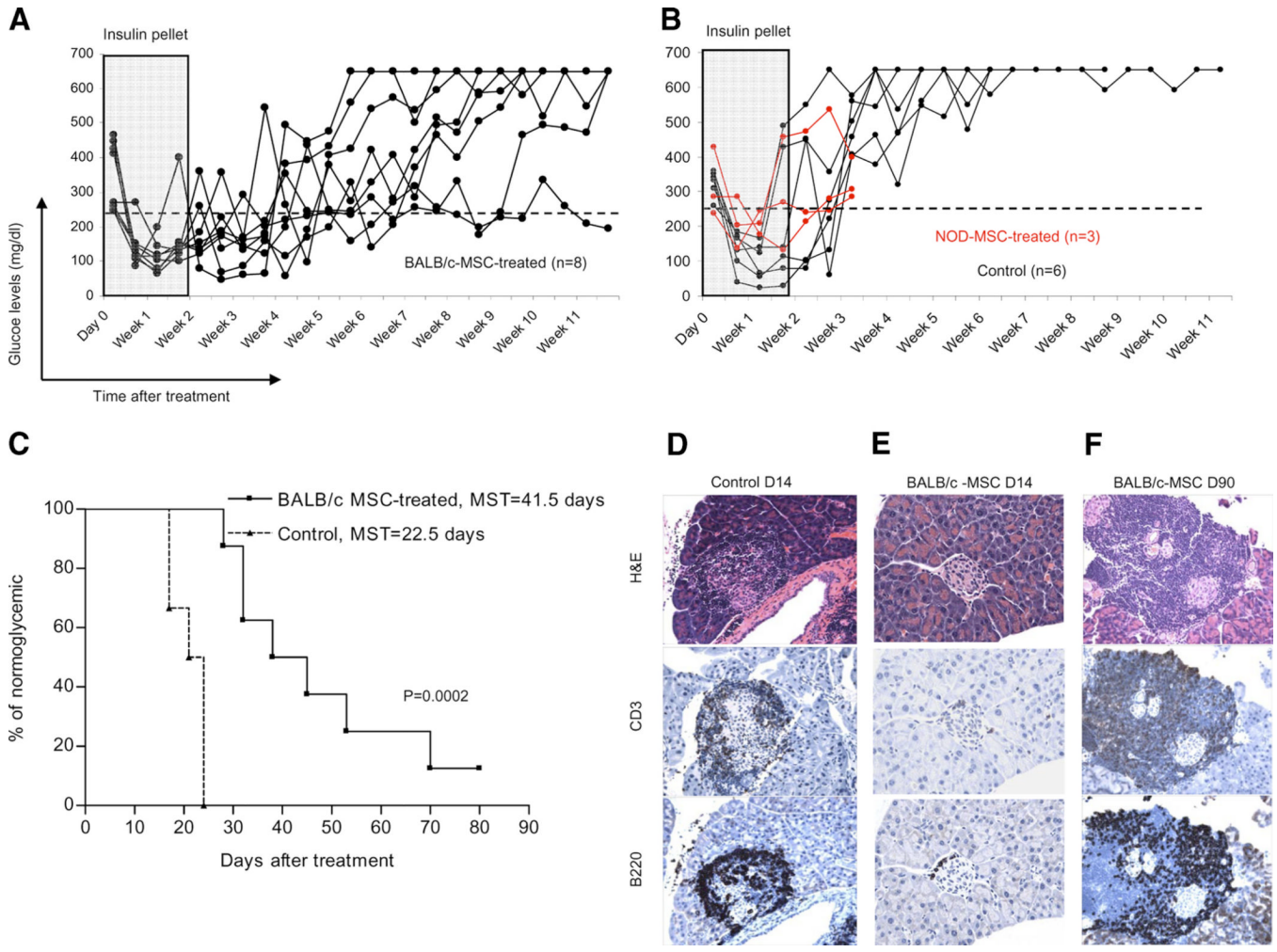

FIGURE 5.

Temporary reversal of diabetes in NOD mice by BALB/c-MSC. The effect of BALB/c- and NOD-MSC on reversing hyperglycemia in new-onset hyperglycemic NOD mice was determined. After the second consecutive hyperglycemic measurement (>250 mg/dl) within 24 h, NOD mice were injected i.v. with 1×10^6 allogeneic BALB/c-MSC or syngeneic NOD-MSC twice a week for 4 wk. Seven of eight BALB/c-MSC-treated mice remained normoglycemic for an average of 41.5 days as compared with 22.5 days for control ($p = 0.0002$), whereas NOD-MSC conferred no protection (*A*–*C*). In the BALB/c-MSC-treated mice 14 days after treatment, islets showed very mild infiltrate confined to the borders of β cells with an almost complete absence of $B220^+$ and $CD3^+$ cells (*E*) compared with the untreated control, which showed a considerable number of $B220^+$ and $CD3^+$ infiltrating cells (*D*). *F*, Ninety days after the onset of hyperglycemia, islets from BALB/c-MSC-treated mouse appeared extensively infiltrated with preserved islet structure.

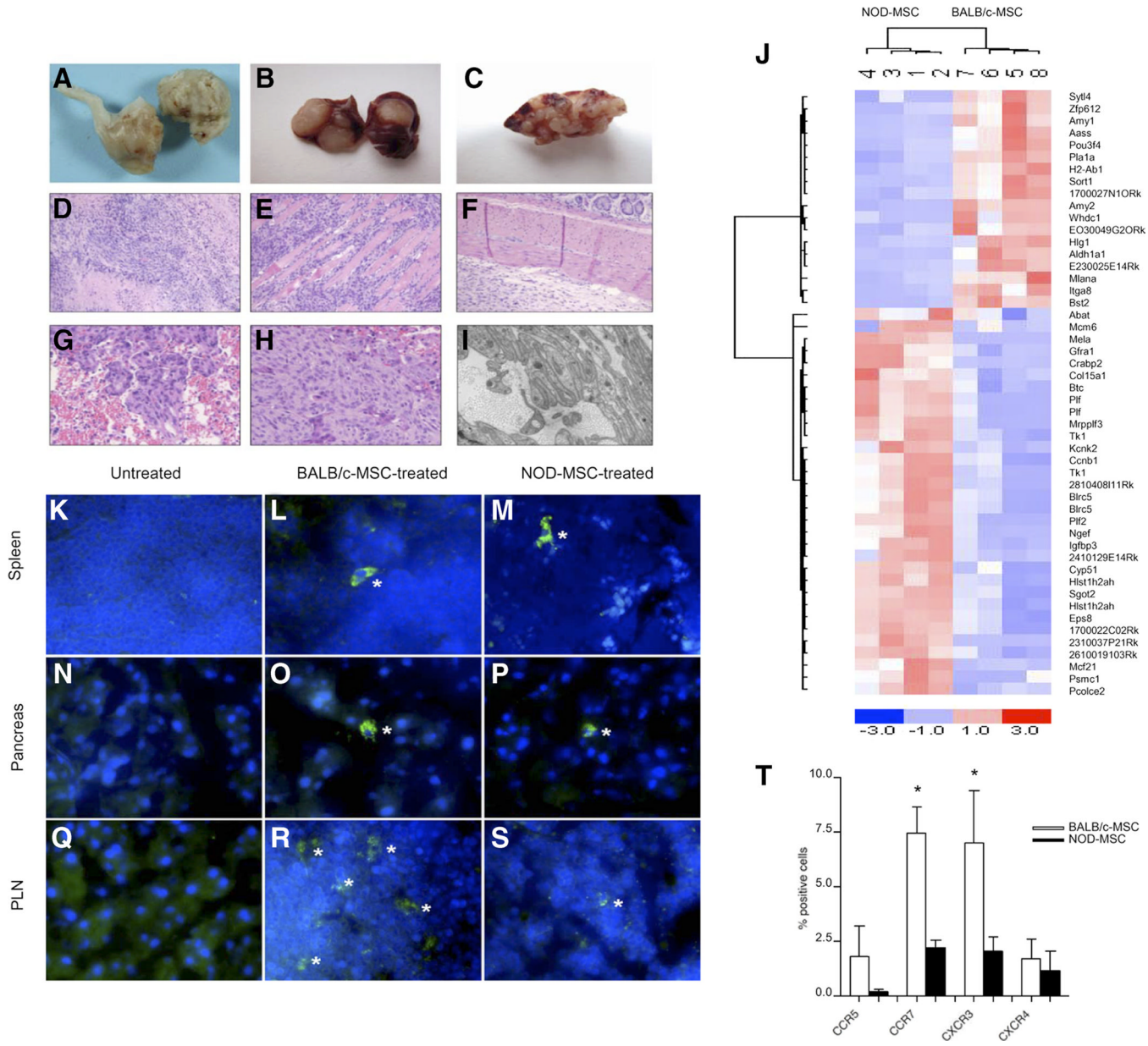

FIGURE 6.

Neoplasia in NOD-MSC-treated mice. The tumor detected in NOD-MSC-treated mice formed nodular masses of 1.5 cm in diameter in the legs of mice, and the tail was completely involved by nodular masses (*A*). Tumors were also identified in the lung and liver as numerous nodules 0.1–0.3 cm in diameter (*B* and *C*). Optical microscopy showed that the malignant tumor was formed of a homogeneous population of malignant spindle cells in sheets and fascicles (400×) (*D*). The tumor invaded muscle, nerve, and annexal structures of the skin and bone (*E*). The tumor also was shown to invade the peritoneum and was located adjacent to the colon (*F*). In the lung, the tumors formed nodular masses with alveolar wall infiltration (*G*) and the tumors in the liver appear as nodular masses (*H*) (×200). Electron microscopy of the hepatic tumor identified compact, intertwined processes covered by basal lamina, consistent with Schwann cell differentiation (*I*) (×19,000). The diagnosis was suggestive of a malignant peripheral nerve sheath tumor. Hierarchical cluster analysis of

differentially expressed genes in NOD- and BALB/c-MSC. Each row represents a single gene (identified by its abbreviation to the right; please refer to Tables I and II for corresponding gene nomenclature). Each column represents the average of four replicates/experiment. Color blocks represent significantly regulated genes (red blocks indicate overexpressed genes and blue blocks indicate underexpressed genes). Color codes at the bottom correlate color intensity with -fold regulation. Analysis of the gene expression profile of NOD- and BALB/c-MSC (obtained from normoglycemic NOD mice and age-matched BALB/c mice) demonstrated that a number of genes, notably several promoting cell cycle and proliferation, were up-regulated in NOD-MSC (sample nos. 5 to 8) vs BALB/c-MSC (sample nos. 1 to 4) (*J*). For a list of genes, please refer to data Tables I and II. Monitoring the trafficking of BALB/c- and NOD-MSC in NOD mice. CFSE-labeled BALB/c- and NOD-MSC were injected into 10-wk-old NOD mice, and at day 3 lymphoid organs and pancreata were examined for the presence of MSC. Spleen (*K*), pancreas (*N*), and PLN (*Q*) from non-injected mice were used as negative controls. MSC distribution was similar in both spleen and pancreas of BALB/c-MSC-treated (*L* and *O*, respectively) and NOD-MSC-treated mice (*M* and *P*, respectively). However, a greater number of BALB/c-MSC (average of 20 cells) was observed in the PLN of NOD mice (*R*) as compared with NOD-MSC-treated animals (two cells) (*S*). Cells were counterstained for 2 min with 300 nM 4’,6-diamidino-2-phenylindole (DAPI) to distinguish nucleated cells. Adjacent sections were collected at a distance of 100 μm. Photographs were taken using a Nikon E-1000 epifluorescence microscope, with a ×40 objective (×400 total magnification). Asterisks indicate CFSE-labeled MSC; CFSE-labeled MSC appear bright green; blue indicates DAPI nuclear counterstaining. Assessment of chemokine receptor expression in MSC by FACS. The expression of CXCR3 and CCR7 was significantly higher in BALB/c-MSC as compared with NOD-MSC ($p = 0.04$ and $p = 0.01$, respectively, data representative of three experiments) (*T*).

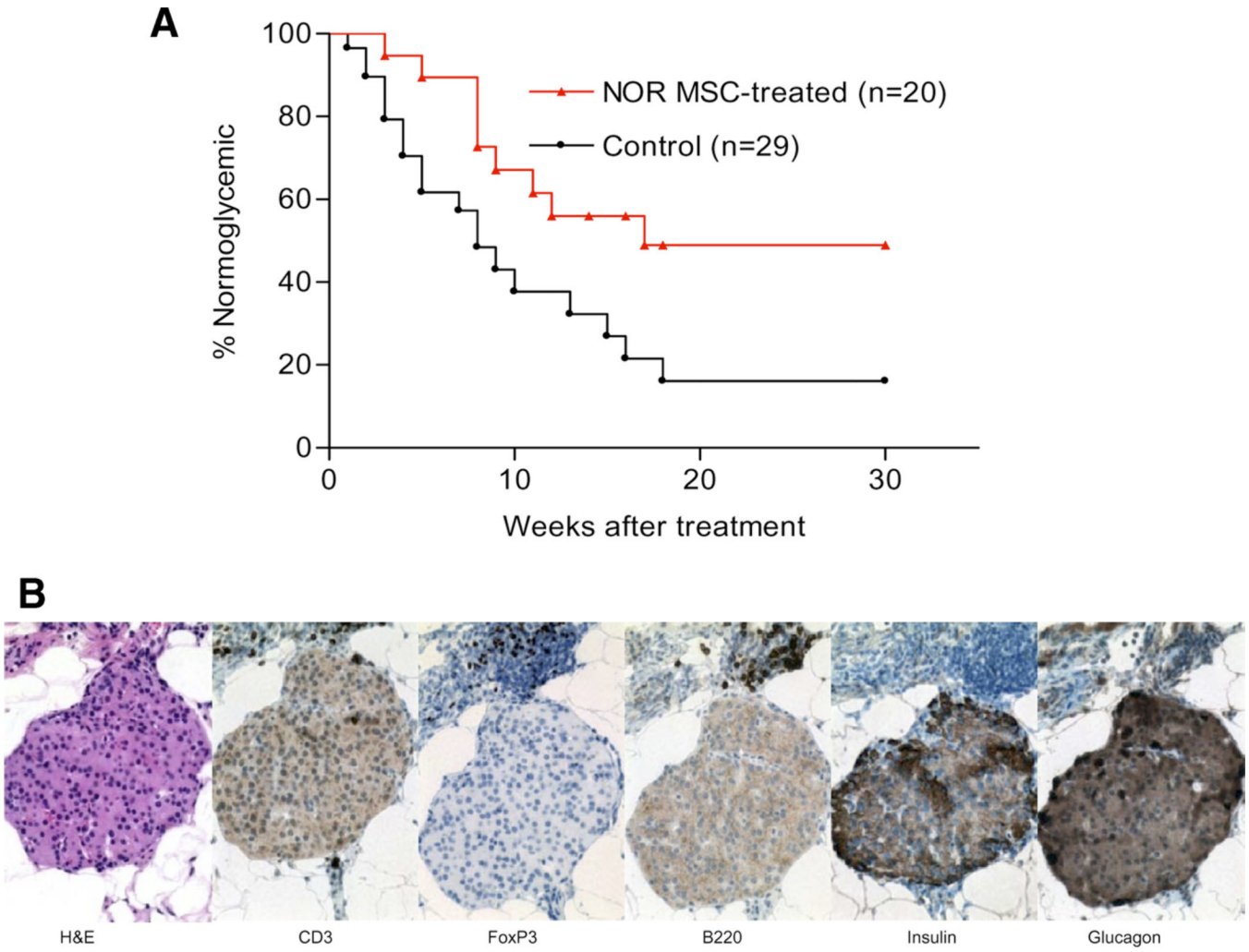

FIGURE 7.

The effect of NOR-MSC in preventing diabetes in NOD mice. NOR-MSC (5×10^5) were injected i.v. into prediabetic female 10-wk-old NOD mice once a week for 4 wk. NOR-MSC were generated from female NOR mice (≤10 wk of age). Occurrence of hyperglycemia was monitored beginning 1 wk after the first injection of MSC and was used to evaluate diabetes development. Compared with untreated NOD, the onset of diabetes was significantly delayed in NOD mice treated with NOR-MSC (*A*). At 30 wk posttreatment, pancre-ata were harvested from NOD mice treated with NOR-MSC. Islet structure was found to be intact with preserved insulin and glucagon staining and little cellular infiltrate (*B*). All photos were taken at 400× original magnification.

Table I

Down-regulated genes in NOD-MSC compared with BALB/c-MSC

Symbol	Name	Function
Whdc1	WAS protein	Not specified
H2-Ab1	Histocompatibility	Ag processing and presentation
Sort1	SORTILIN, SORT1	Cell differentiation
Zfp612	Zinc finger protein 612	Regulation of transcription, DNA-dependent
Aldh1a1	Aldehyde dehydrogenase family	Morphogenesis
		Metabolic process
		Oxidation reduction
		Positive regulation of apoptosis
		Retinoic acid metabolic process
Amy1	Amylase 1	Carbohydrate metabolic process
Amy2	Pancreatic amylase 2	Carbohydrate metabolic process
E030049G20Rik	E030049G20Rik	Not specified
E230025E14Rik	Erythrocyte protein band	Mesoderm development
Itga8	Integrin α 8	Cell adhesion and differentiation and matrix organization and biogenesis
		Positive regulation of TGFβ signaling pathway
Aass	Aminoadipate-semialdehyde synthase	Generation of precursor metabolites and energy
Bst2	Bone marrow stromal cell Ag 2	Not specified
Hig1	HIG1 domain family	Response to stress
Pla1a	Phospholipase A1	Lipid catabolic process
Abat	4-aminobutyrate aminotransferase	Neurotransmitter catabolic process
1700027N10Rik	RIKEN cDNA 1700027N10 gene	Not specified
Mlana	Melanoma-associated Ag	Not specified
Sytl4	Synaptotagmin-like 4	Intracellular protein transport
Pou3f4	POU domain, class 3, transcription factor 4	Morphogenesis

Table II

Up-regulated genes in NOD-MSC compared with BALB/c-MSC

Symbol	Name	Function
Plf	Prolactin family	Positive regulation of neuroblast proliferation
Plf2	Prolactin family 2	Positive regulation of cell proliferation
Hist1h2ah	Histone cluster	Nucleosome assembly
Mrpplf3	Mitogen regulated protein	Biological process
2310037P21Rik	Transmembrane protein 158	Not specified
Mela	Melanoma antigen	DNA recombination
Tk1	Thymidine kinase 1	DNA replication
2610019I03Rik	Centromere protein M proliferation-associated nuclear element 1	Not specified
Mcm6	Mini-chromosome maintenance-deficient 6	DNA replication
Birc5	Baculoviral IAP repeat-containing 5	Anti-apoptosis
Cyp51	Cytochrome P450	Cholesterol biosynthetic process
Igfbp3	Insulin-like growth factor-binding protein 3	Regulation of cell growth
2410129E14Rik	Tubulin	Microtubule-based movement
Col15a1	Collagen, type XV, α 1	Cell adhesion
Gfra1	Glial cell line derived neurotrophic factor family receptor α 1	Nervous system development
		Tyrosine kinase signaling pathway
Kcnk2	Potassium channel, subfamily K, member 2	G-protein-coupled receptor protein-signaling pathway
Psmc1	Protease (prosome, macropain) 26S subunit	Protein catabolic process
Ngef	Neuronal guanine nucleotide exchange factor	Neural cell development and differentiation
Sgol2	Shugoshin-like 2	Cell cycle
Crabp2	Cellular retinoic acid binding protein II	Embryonic forelimb morphogenesis
Btc	Epidermal growth factor family member	Cell proliferation
Eps8	Epidermal growth factor receptor pathway substrate 8	Proteolysis
Mcf2l	Mcf.2 transforming sequence-like	Regulation of Rho protein signal transduction
Pcolce2	Procollagen C-endopeptidase enhancer 2	Not specified
Ccnb1	Cyclin B1	Cell cycle
1700022C02Rik	Centromere protein P	Not specified